Agricultural and Environmental Chemistry

Synthesis and Pesticidal Activities of New Quinoxalines

Xing-Hai Liu, Wei Yu, Li-Jing Min, David E. Wedge, Cheng-Xia Tan, Jian-Quan Weng, Hong-Ke Wu, Dr. Charles L. Cantrell, Joanna Bajsa-Hischel, Xue-Wen Hua, and Stephen O. Duke

J. Agric. Food Chem., **Just Accepted Manuscript** • DOI: 10.1021/acs.jafc.0c01042 • Publication Date (Web): 12 Jun 2020

Synthesis and Pesticidal Activities of New Quinoxalines

Xing-Hai Liu[1*], Wei Yu[1], Li-Jing Min[2], David E. Wedge[3], Cheng-Xia Tan[1], Jian-Quan Weng[1], Hong-Ke Wu[1], Charles L. Cantrell[3], Joanna Bajsa-Hirschel[3], Xue-Wen Hua[5], and Stephen O. Duke[4*]

1.College of Chemical Engineering, Research Institue of Pesticide, Zhejiang University of Technology, Hangzhou, 310014, China

2. Key Laboratory of Vector Biology and Pathogen Control of Zhejiang Province, College of Life Science, Huzhou University, Huzhou Cent. Hosp., Huzhou, 313000, Zhejiang, China

3. Natural Products Utilization Research Unit, USDA-ARS University, MS 38677, USA

4. National Center for Natural Product Research(NCNPR), School of Pharmacy, University of Mississippi, University, MS, 38677, USA

5. College of Agriculture, Liaocheng University, 252000, Liaocheng, Shandong, China

Abstract: Natural products are a source of many novel compounds with biological activity for discovery of new pesticides and pharmaceuticals. Quinoxaline is a fused *N*-heterocycle in many natural products and synthetic compounds, seven novel quinoxaline derivatives were designed and synthesized *via* three steps. Pesticidal activities of title quinoxaline derivatives were bioassayed. Most of these compounds had herbicidal, fungicidal, and insecticidal activities. The compounds 2-(6-methoxy-2-oxo-3-phenylquinoxalin-1(2*H*)-yl)acetonitrile(**3f**) and

1-allyl-6-methoxy-3-phenylquinoxalin-2(1*H*)-one (**3g**) were the most active herbicides and fungicides. Mode of action studies indicated that **3f** is a protoprophyrinogen oxidase-inhibiting herbicide. Compound **3f** also possessed broad-spectrum fungicidal activity against the plant pathogen *Colletotrichum* species. Some of these compounds also had insecticidal activity. Molecular docking and DFT analysis can potentially be used to design more active compounds.

Keywords: Quinoxaline; herbicidal; fungicidal; insecticidal; DFT; molecular docking

INTRODUCTION

Pesticides are important tools to protect crops, increase yields and quality in agriculture. New pesticide discovery can be from natural products. Benzopyrazine(quinoxaline) is a fused N-heterocycle found in many natural compounds (Figure **1**), such as the cyclic peptide triostin A,[1] izumiphenazines A–C,[2] hunanamycin A[3,4], and vitamin B2.[5,6] Quinomycins are a type of cyclic oligopeptide antibiotic containing the quinoxaline group in the macrocycles. Izumiphenazines A-C with the quinoxaline group were isolated from *Streptomyces* species. The natural product hunanamycin A with a quinoxaline moiety, was isolated from *Bacillus hunanensis*. Currently, synthetic quinoxaline derivatives possess a diversity of activities, such as antibacterial,[7] anti-ebola,[8] antileishmanial,[9] antitubercular,[10] antifungal,[11] antimalarial,[12] anticancer,[13] and antineoplastic activities[14]. The quinoxaline motif also exists infunctional materials, including organic dyes[15] and DNA cleavage agents.[16-19]

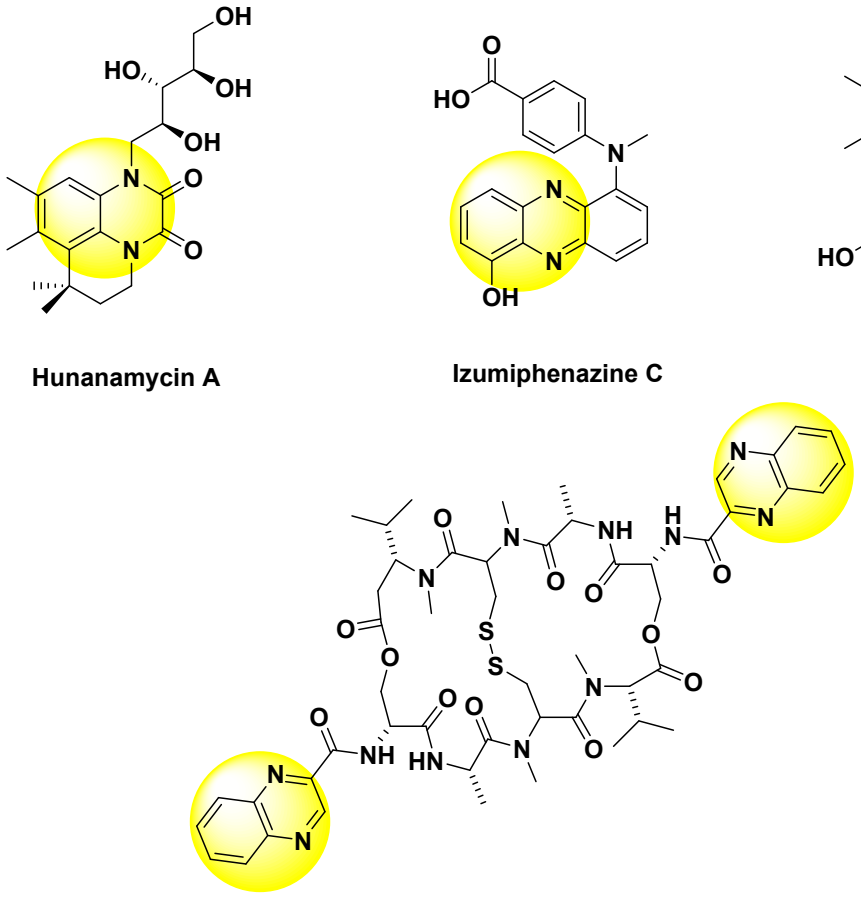

Figure **1** Some natural products with the quinoxaline moiety

However, the quinoxaline(or pyrazine) moiety has had little application in industrial and agricultural fields. Some patents[20-22] reported the quinoxaline derivatives were used as herbicides or herbicide safener. Thus far, only the herbicides diquat, quizalofop-p-methyl, and quizalofop-p-tefuryl, the fungicide pyraziflumid, and the insecticide chinomethionat(Figure **2**) are commercial pesticides with the quinoxaline or pyrazine moiety.

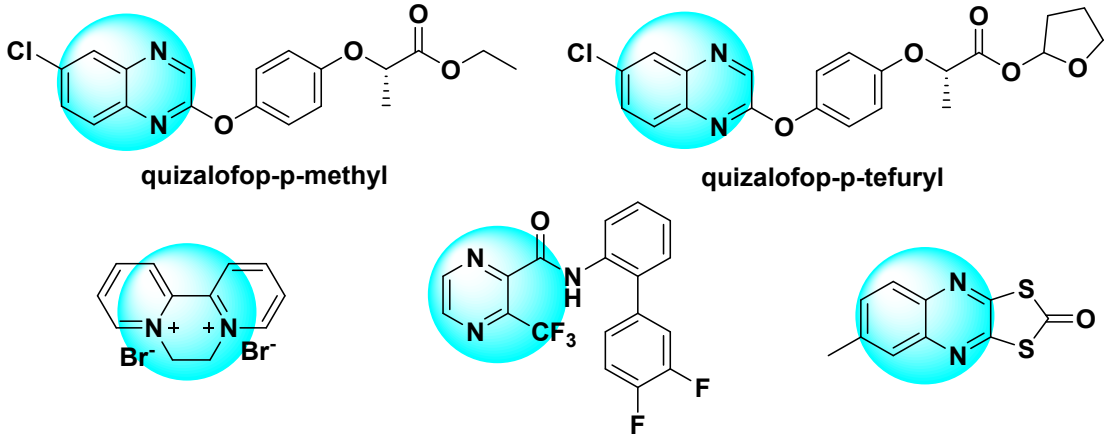

Figure 2 Representative pesticides with the pyrazine moiety

In our previous work, many nitrogen-containing heterocycles with pesticidal activity were designed and synthesized.[23-34] For the above reason, to discover active lead compounds, we designed some quinoxaline compounds with a flexible side chain. Some of the synthetic quinoxaline derivatives exhibited good herbicidal, fungicidal and mosquitocidal activity.

MATERIALS AND METHODS

Instruments.

Melting points(m.p.) were tested on an X-4 digital melting point instument(Gongyi, China) and the temperature was uncorrected. FT-IR was measured on a Nocolet 670 fourier transform infrared spectrometer(Thermofisher, USA). ^{1}H NMR spectra were tested on an AP-500 nuclear magnetic resonance spectrometer(Bruker, Germany). ESI-HR-MS were tested on time-of-flight mass

spectrometer (Agilent 6520, MA, USA or Jeol Accu TOF 4G, Tokyo, Japan). All the reagents were freshly prepared or purchased from chemical company.

Synthesis

4-methoxybenzene-1,2-diamine(1)

To a mixture of 4-methoxy-2-nitroaniline (0.1 mol), $NH_2NH_2 \cdot H_2O$ (85%, 75 mL) in MeOH (40 mL), Raney Ni (0.4 mol) was added slowly, then refluxed. The residue Raney Ni was filtrated and the solvent MeOH was evaporated to afford light brown crystal **1**.

7-Methoxy-3-phenylquinoxalin-2(1*H*)-one(2)

To a solution of 4-methoxybenzene-1,2-diamine (0.1 mol) in EtOH (100 mL), methyl 2-oxo-2-phenylacetate (0.1 mol) was added and then further stirred for another 1 h. A yellow solid was produced in good yield. 7-Methoxy-3-phenylquinoxalin-2(1*H*)-one, yield 95.6%, m.p. 180-183℃, ^{1}H NMR(500MHz, $CDCl_3$) δ: 8.43(m, 2H, Ph-H), 7.54(m, 3H, Ph-H), 7.41(d, *J*=2.7Hz, 1H, Ph-H), 7.30 (s, 1H, Ph-H), 7.20 (d, *J*=2.7Hz, 1H, Ph-H), 3.92(s, 3H, OCH_3).

General procedure for compounds 3a to 3g

7-Methoxy-3-phenylquinoxalin-2(1*H*)-one (1.26 g, 0.005 mol) and dried potassium carbonate (0.2 g, 0.0056 mol) was dissolved in DMF (15 mL) and stirred for 10 min, then different RCl (0.005 mol) was dropwised, and magnetic stirred for overnight. Then the reaction solution was poured into ice H_2O, a lot of solid was given, then filtered, recrystallized and dried to give **3a~3g** in good yields.

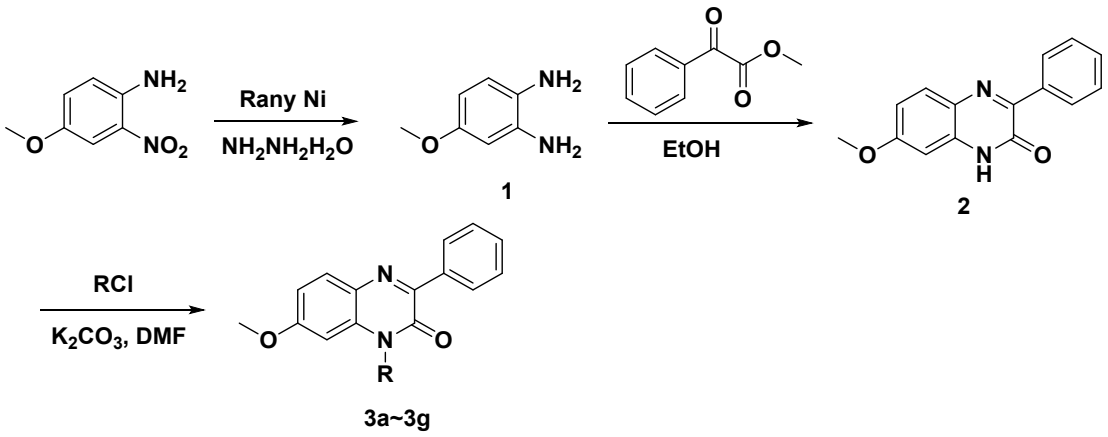

Scheme 1. The synthetic pathway of quinoxaline derivatives

4-((7-methoxy-2-oxo-3-phenylquinoxalin-1(2H)-yl)methyl)benzonitrile ***3a***

Yellow solid, m.p. 148-151℃, yield 62.3%, FT-IR (KBr, ν_{max}, cm^{-1}): 2922.24, 2225.96(C≡N), 1649.83(C=O), 1496.97, 1444.59, 1382.91, 1286.68, 1269.43, 1038.01, 809.97, 692.59, 545.98; ^1H NMR (500 MHz, $CDCl_3$) δ: 8.37-8.33 (m, 2H, Ph-H), 7.66-7.63 (m, 2H, Ph-H), 7.52-7.48 (m, 4H, Ph-H), 7.41 (d, *J* = 8.5 Hz, 2H, Ph-H), 7.12-7.08 (m, 1H, Ph-H), 6.95 (dd, *J* = 8.9, 2.5 Hz, 1H, Ph-H), 5.60 (s, 2H, -CH_2), 3.89 (s, 3H, -OMe); ESI-HRMS calcd for $C_{23}H_{17}N_3O_2$ 368.1394, found 368.1399$[M+H]^+$.

1-(4-(tert-butyl)benzyl)-7-methoxy-3-phenylquinoxalin-2(1H)-one ***3b***

Yellow solid, m.p. 86-89℃, yield 68.2%, FT-IR (KBr, ν_{max}, cm^{-1}): 2959.18, 1643.96(C=O), 1611.39, 1580.18, 1499.00, 1441.01, 1383.51, 1269.28, 1215.24, 1165.16, 1025.94, 812.85, 693.96, 600.44, 530.20; ^1H NMR (500 MHz, $CDCl_3$) δ: 8.38-8.34 (m, 2H, Ph-H), 7.49-7.45 (m, 3H, Ph-H), 7.42 (d, *J* = 2.9 Hz, 1H, Ph-H), 7.33-7.30 (m, 2H, Ph-H), 7.26-7.21 (m, 3H, Ph-H), 7.10 (dd, *J* = 9.2, 2.9 Hz, 1H, Ph-H), 5.52 (s, 2H, -CH_2), 3.88 (s, 3H, -OMe), 1.27 (s, 9H, -Bu); ESI-HRMS calcd for $C_{26}H_{26}N_2O_2$ 399.2067, found 399.2066$[M+H]^+$.

1-(4-bromobenzyl)-7-methoxy-3-phenylquinoxalin-2(1H)-one ***3c***

Yellow solid, m.p. 131-132℃, yield 72.4%, FT-IR (KBr, ν_{max}, cm^{-1}): 2926.92, 1649.98(C=O), 1572.67, 1490.75, 1444.94, 1384.19, 1266.04, 1210.18, 1174.08, 1070.73, 1032.79, 807.27, 756.52, 689.57, 622.97, 536.01, 477.70; ^{1}H NMR (500 MHz, $CDCl_3$) δ: 8.37-8.33 (m, 2H, Ph-H), 7.52-7.48 (m, 4H, Ph-H), 7.43 (d, *J* = 2.3 Hz, 2H, Ph-H), 7.17 (dd, *J* = 12.5, 4.0 Hz, 3H, Ph-H), 7.09 (dd, *J* = 9.2, 2.8 Hz, 1H, Ph-H), 5.50 (s, 2H, -CH_2), 3.88 (s, 3H, -OMe); ESI-HRMS calcd for $C_{22}H_{17}BrN_2O_2$ 421.0546, found 421.0551 $[M+H]^+$.

3-((7-methoxy-2-oxo-3-phenylquinoxalin-1(2H)-yl)methyl)benzonitrile ***3d***

Yellow solid, m.p. 157-159℃, yield 57.6%, FT-IR (KBr, ν_{max}, cm^{-1}): 2226.42(C≡N), 1647.55(C=O), 1610.21, 1496.28, 1441.92, 1383.41, 1285.65, 1244.28, 1161.20, 1038.81, 809.56, 692.91, 599.15, 544.89; ^{1}H NMR (500 MHz, $CDCl_3$) δ: 8.38-8.33 (m, 2H, Ph-H), 7.64-7.61 (m, 2H, Ph-H), 7.53-7.47 (m, 4H, Ph-H), 7.39 (d, *J* = 8.5 Hz, 2H, Ph-H), 7.12-7.06 (m, 2H, Ph-H), 5.60 (s, 2H, -CH_2), 3.89 (s, 3H, -OMe); ESI-HRMS calcd for $C_{23}H_{17}N_3O_2$ 368.1394, found 368.1398$[M+H]^+$.

1-((2-chlorothiazol-5-yl)methyl)-7-methoxy-3-phenylquinoxalin-2(1H)-one ***3e***

Yellow solid, m.p. 158-160℃, yield 46.4%, FT-IR (KBr, ν_{max}, cm^{-1}): 2950.98, 1638.52(C=O), 1606.75, 1497.40, 1445.68, 1383.15, 1266.30, 1221.31, 1028.05, 927.23, 813.12, 693.36, 626.30, 540.82; ^{1}H NMR (500 MHz, $CDCl_3$) δ: 8.37-8.31 (m, 2H, Ph-H), 7.69 (s, 1H, thiazole-H), 7.55-7.50 (m, 4H, Ph-H), 7.37 (d, *J* = 9.2 Hz, 1H, Ph-H), 7.24 (dd, *J* = 9.1, 2.9 Hz, 1H, Ph-H), 5.56 (s, 2H, -CH_2), 3.92 (s, 3H, -OMe); ESI-HRMS calcd for $C_{19}H_{14}ClN_3O_2S$ 384.0568, found 384.0571 $[M+H]^+$.

2-(7-methoxy-2-oxo-3-phenylquinoxalin-1(2H)-yl)acetonitrile ***3f***

Yellow solid, m.p. 123-126℃, yield 45.1%, FT-IR (KBr, ν_{max}, cm^{-1}): 2921.19, 2259.19(C≡N), 1645.58(C=O), 1612.63, 1499.88, 1384.14, 1283.15, 1165.78, 1070.69, 801.90, 689.50, 622.17, 531.38; ^1H NMR (500 MHz, $CDCl_3$) δ: 8.34-8.30 (m, 2H, Ph-H), 7.53-7.49 (m, 4H, Ph-H), 7.28 (d, *J* = 1.1 Hz, 2H, Ph-H), 5.27 (s, 2H, -CH_2), 3.94 (s, 3H, -OCH_3); ESI-HRMS calcd for $C_{17}H_{13}N_3O_2$ 292.1081, found 292.1087 $[M+H]^+$.

1-allyl-7-methoxy-3-phenylquinoxalin-2(1H)-one ***3g***

Yellow solid, m.p. 91-94℃, yield 52.3%, FT-IR (KBr, ν_{max}, cm^{-1}): 2922.09, 2851.01, 1636.25, 1612.38(C=O), 1572.77, 1495.47, 1413.09, 1383.33, 1288.92, 1268.37, 1055.61, 807.86, 688.34, 539.55; ^1H NMR (500 MHz, $CDCl_3$) δ: 8.36-8.32 (m, 2H, Ph-H) , 7.52-7.47 (m, 4H, Ph-H), 7.25 (d, *J* = 9.2 Hz, 1H, Ph-H), 7.18 (dd, *J* = 9.2, 2.9 Hz, 1H, Ph-H), 6.00-5.93 (m, 1H, -CH), 5.29-5.21 (m, 2H, =CH_2), 5.00-4.97 (m, 2H, -CH_2), 3.92 (s, 3H, -OCH_3); ESI-HRMS calcd for $C_{18}H_{16}N_2O_2$ 293.1285, found 293.1292 $[M+H]^+$.

Herbicide Bioassays

Lettuce and Bentgrass

Previously published bioassays for herbicidal activity using *Lactuca sativa* L.(lettuce, Iceberg A Crisphead cultivar from Burpee Seeds, Warminster, PA, USA) and *Agrostis stolonifera* L. (bentgrass, Penncross variety from Turf-Seed, Inc. of Hubbard, OR, USA) were used.[35] Briefly, seeds of bentgrass and lettuce were surface sterilized for 10 min with a 0.5% to 1% (v/v) solution of NaOCl, rinsed with deionized H_2O, and then dried in a semi-sterile environment. A 1.5-cm Whatman Grade 1 filter paper disc was putted into 24-well plate. Every wells contained 200 μL control solution(deionized H_2O, 200 μL), control solvent(deionized H_2O, 180 μL+ test compound

149 solvent, 20 μL) or samples (deionized H_2O, 180 μL+ sample, 20 μL). Deionized H_2O was putted
150 into the wells before solvent or samples. Samples were dissolved in CH_3COCH_3. Ten mg of
151 bentgrass seeds or five lettuce seeds or were putted into each 24-well for the bioassays, and then
152 sealed the plate by using Parafilm. These 24-well plates were incubated[(bentgrass, 12 days) and
153 (lettuce, 5 days)] in a CU-36L5 Percival Scientific (Perry, IA, USA) incubator. Temperature and
154 light conditions were continuous light (120 $\mu mol \cdot s^{-1} \cdot m^{-2}$) at 26 °C. Phytotoxicity of control
155 solvent or samples was quantitated 0-5 grade: 5 is no germination of the seeds, 4 is more than 50%
156 germination of the seeds, 3 is about 50% germination of the seeds, 2 is less than 50% germination
157 of the seeds, 1 is some stunting to the seedlings, but no inhibition of germination and 0 is no
158 effect. Each experiment was repeated twice.

159 ***Duckweed***

160 A previously published bioassay with duckweed (*Lemna paucicostata* Hegelm.) was used.[36] A
161 single colony consisting of a mother and two daughter fronds was used to establish duckweed
162 stocks that were grown in Hoagland media (pH=5.5) in sterile jars with vented lids in a CU-36L5
163 Percival Scientific incubator. Hoagland media were changed every 2 to 3 days. Duckweed
164 experiments were carried out by using non-pyrogenic polystyrene 6-well plates (CoStar 3506,
165 Corning Incorporated). Each well contained H_2O (50 μL), or CH_3COCH_3 (50 μL), or test
166 compound (50 μL) plus 4950 μL of the Hoagland's media. The doubling time of frond area was
167 approximately 1 to 1.5 day. Then two, three-frond plants(four- to five-days-old) was inoculated
168 into each well and repeated 3 times. Growth was determined by image analysis of graphic
169 templates of the 6-well plates using LemnaTec (LemnaTec, Würselen, Germany) hardware and

software. Total frond area, frond color (necrotic or chlorotic effects) and frond number were recorded every day. R statistics software was used to determine IC_{50} values.[37]

Electrolyte-Leakage

The effect of pure compound **3f** on plasma membrane stability was determinedon cucumber-cotyledon discs using a previously published method.[38] Under dim green light, cucumber cotyledon discs (4 mm) were cut, and 50 discs were floated in Petri plates (sterile, 6 × 1.5 cm, polystyrene) containing 4850 µL of 1 µM MES buffer (pH=6.5) with 2% sucrose plus CH_3COCH_3 (150 µL) or test samples solution (150 µL). Compound **3f**, **3g**, the positive control acifluorfen, clomazone and solvent control (CH_3COCH_3) was tested for three times at 10 µM, 33 µM, 100 µM, 333 µM and 1 mM. Acifluorfen causes rapid plasma-membrane leakage in the light due to its activity as a protoporphyrinogen oxidase (PPO) inhbitor.[38] At the beginning of the experiment, 55 discs were placed in test tubes with buffer (5 mL). These tubes were placed in boiling H_2O for 15 min and then cooled to 20 ^oC, after which electrical conductivity was determined at 0-h. Then the dishes was placed under 18-h dark incubation. After that, electrical conductivity was determined at 19, 20, 22, and 24 h under high light intensity condition. The graphs of electrical conductivity vs time were drawn from these data. The maximal possible electrical conductivity was tested by the measurement of the electrical-conductivity of the solution in which the cotyledon discs were boiled.

Porphyrin-Dependent Activity

To determine if the leakage caused by **3f** is due to production of a porphyrin, the experiment of Lydon and Duke[39] was conducted in which the porphyrin synthesis inhibitor gabaculine was used with the herbicide. The PPO inhibitor acifluorfen was used as a positive control. Gabaculine itself

has no significant effect in this bioassay. Reduction of the herbicide-caused electrolyte leakage by gabaculine occurs with PPO inhibitors, such as acifluorfen.

Fungicide Bioassay

Direct bioautography, a simple method to screen samples for fungicide activity,[40] as used as a fungicide bioassay. Standards at 2 mM in EtOH (95%) were spotted on plates in 8 µL droplets. Pure test samples were prepared in 95% ethanol at 20 mg/mL and 8 µL of each was spotted on plates. Compounds **3a**~**3g** and the commercial fungicide captan were tested for fungicidal activity against *Colletotrichum gloeosporioides*, *Colletotrichum fragariae* and *Colletotrichum acutatum* (all strawberry anthracnose-causing plant pathogens) using direct overlay bioautography. Following sample application and solvent evaporation, each TLC plate was sprayed spore suspension of above three fungus (*C. gloeosporioides*, *C. fragariae* and *C. acutatum*) with the concentration of 3.0×10^5 spores/mL, then the plate was incubated for 4 days at 26°C in a moisture chamber with a 12-h photoperiod. Clear zones or diffuse zones of three fungal growth inhibitions on the TLC plate indicated the effective of fungicidal activity for pure compound.

Mosquito Bioassay

Larval *Aedes aegypti* (Orlando strain) was provided by the USDA/ARS/CMAVE in Gainesville, FL, US. This strain has never been supplemented with additional wild type mosquitoes since initial collection in 1952 in Orlando, Florida. Production and maintenance procedures for mass rearing had been reported previously.[41,42]

Larval *Aedes aegypti* activity was carried out following standard protocols and have been described previously.[43,44] Compounds **3a**~**3g** were initially diluted in dimethyl sulfoxide or EtOH to make 100 µg/µL stock solutions. Stocks of compounds **3a**~**3g** were diluted to 200 µL for larval

bioassays. At last, the larval bioassays was determiend against five 1st instar *Ae. aegypti* at 1, 0.5, 0.25 and 0.1 μg/μL, respectively. The negative controls was untreated while positive control used was permethrin. The larval *Aedes aegypti* was judged as dead if it was no response to probing with the tip of a pipette after 24 h. The experiments were done for three times on different days.

Molecular Docking

The structure of *Nicotiana tabacum* PPO (PDB ID: 1SEZ) was downloaded from protein data bank (PDB). The protein crystal structure *Nicotiana tabacum* PPO and the small molecule 2-((7-methoxy-3-phenylquinoxalin-2-yl)oxy)acetonitrile **3f** were prepared by standard methods using the discovery studio 2.5. After molecular docking, the best binding mode was selected according to the results of docking energy, compared with the ligand in the *Nt*PPO.

Density Functional Theory Analysis

According to the bioassay results, high active compound **3f** and low active compound **3c** were selected and drawn in Gaussview 5.0 and the two structures optimized using DFT-B3LYP/6-31G methods in Gaussian 03 software.[45] The two optimized geometries are at the minimal point on the potential surface according to no imaginary frequencies.

RESULTS AND DISCUSSION

Synthesis and Spectra

The synthetic route of quinoxaline derivatives is outlined in Scheme **1**. Quinoxaline is an important skeleton in many natural products. There are two classic synthetic methods. In our work, the quinoxaline ring was synthesized using diamine and dione as reaction materials. In the process of preparing final quinoxaline derivatives, we found two isomers. The main product is the O-alkyl

product. The title seven quinoxaline derivatives were confirmed by FT-IR, ^{1}H NMR and HR-ESI-MS. In the ^{1}H NMR spectra of synthesized quinoxaline derivatives, all the –CH_2 proton signals were found around 5 ppm. The signals around 3.9 ppm can be assigned as the proton of OCH_3 group. Meanwhile, all of the synthesized quinoxaline derivatives displayed $[M+H]^+$ peak in the HR-ESI-MS results, which is same as the theoretical values.

Biological Activity

Herbicidal Activity

All the compounds were tested against lettuce and bentgrass at 1 mM. This bioassay determines phytotoxicity of compounds against a dicotyledonous (lettuce) and a monocotyledonous (bentgrass) plant species. At 1 mM, all the compounds had good phytotoxic effects. Compounds **3f** and **3g**, had the best activity against creeping bentgrass (ranking 4) and lettuce (ranking 5). The leaf of lettuce was bleached by compound **3f**. Compounds **3d** and **3e** had good activity against the two species (ranking 4 on both). Compounds **3a, 3b** and **3c** had moderate activity against lettuce, and weak activity against bentgrass. Among them, the herbicidal activity of compound **3f** (ranking 5) and **3g** (ranking 5) against the lettuce was the same as the positive control **c**lomazone at 1 mM, but a little weaker (ranking 4) than acifluorfen (ranking 5) against the bentgrass.

In the dose-response bioassays on duckweed, the two most active compounds against lettuce and bentgrass (**3f** and **3g)** were tested, and the IC_{50} values were 13.99±3.17 and 24.56±10.02 μM for compounds **3f** and **3g**, respectively (Table 1). For the commercial bleach herbicide clomazone and acifluorfen acid, the IC_{50} values were 126.10 ± 18.87 μM and 0.73 ± 0.09 μM, respectively. IC_{50} values of compounds **3f** and **3g** were better than the commercial carotenoid synthesis-inhibiting herbicide clomazone (126.10 ± 18.87 μM) and weaker than the other commercial PPO inhibitor herbicide acifluorfen (0.73 ± 0.09 μM) in the same bioassay. Although their modes of action are

different, clomazone and acifluorfen both cause foliar bleaching. From the herbicidal activity against lettuce and creeping bentgrass, it is obvious that the substituent R has a very large effect on the activity. When the substitution is a substituted benzene ring, the herbicidal trend of the compounds was alkyl>heterocycle>substituted benzene. Among these compounds, the $CNCH_2$ provides the best activity and causes foliar bleaching. This may be because the CN group interacts with a critical amino acid residue of PPO, because, in the simulated molecular docking, the CN group interacted with Thr 176 via hydrogen bonding.

Table **1** The phytotoxicity of seven compounds against three plant species

No.	R	Lettuce	Agrostis	Duckweed(IC_{50}(μM))
3a	4-$CNPhCH_2$	3	1	-
3b	4-*t*-$BuPhCH_2$	3	1	-
3c	4-Br $PhCH_2$	2	1	-
3d	3-$CNPhCH_2$	4	3	-
3e	2-Cl-thiazole-5-CH_2	4	3	-
3f	$CNCH_2$	5*	4	13.99±3.17
3g	CH_2=$CHCH_2$	5	4	24.56±10.02
Clomazone		5	5	126.10 ± 18.87
Acifluorfen		5	5	0.73 ± 0.09

0 = no effect and 5 = no germination of the seeds.

*bleached

272 ***Electrolyte-Leakage Assay***

273 PPO inhibitors all cause rapid loss of cellular electrolytes and bleaching of chloroplast pigments
274 by the photodynamic action of protoporphyin IX that accumulates when PPO is inhibited. Because
275 bleaching was observed with **3f** in lettuce, an electrolyte leakage assay was done with acifluorfen
276 as a positive control. Compound **3f** caused light-dependent electrolyte leakage (Figure 3). These
277 results are similar to those caused by commercial PPO inhibitor herbicides like acifluorfen. The
278 effects of **3f** at 100 μM was similar to the effect of acifluorfen at 33 μM. The fact that the
279 compound **3f** compromises membrane integrity indicates that the mechanism of action of this
280 compound is directly related to cell membrane damage like that of PPO inhibitors.

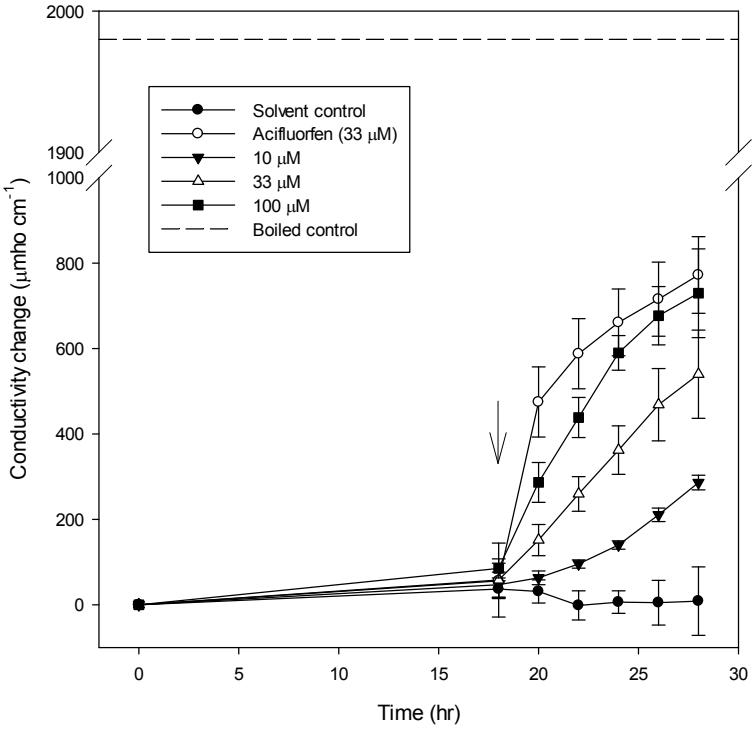

281

282 Figure 3. The electrolyte-leakage of cucumber cotyledon discs caused by compound **3f** at different
283 concentrations. The arrow indicates exposure to light. Error bars are ± 1SE. Dotted line is
284 conductivity of boiled discs (maximum possible effect).

Gabaculine inhibits the porphyrin pathway at an early stage, preventing the accumulation of proporphyin IX caused by PPO inhibitors.[39] Gabaculine reversed the effect of **3f** and acifluorfen on cucumber cotyledon disc leakage (Figure 4). Reversal was with acifluorfen was similar to that reported previously.[36] The results with gabaculine reversal indicate that **3f** is a PPO inhibitor.

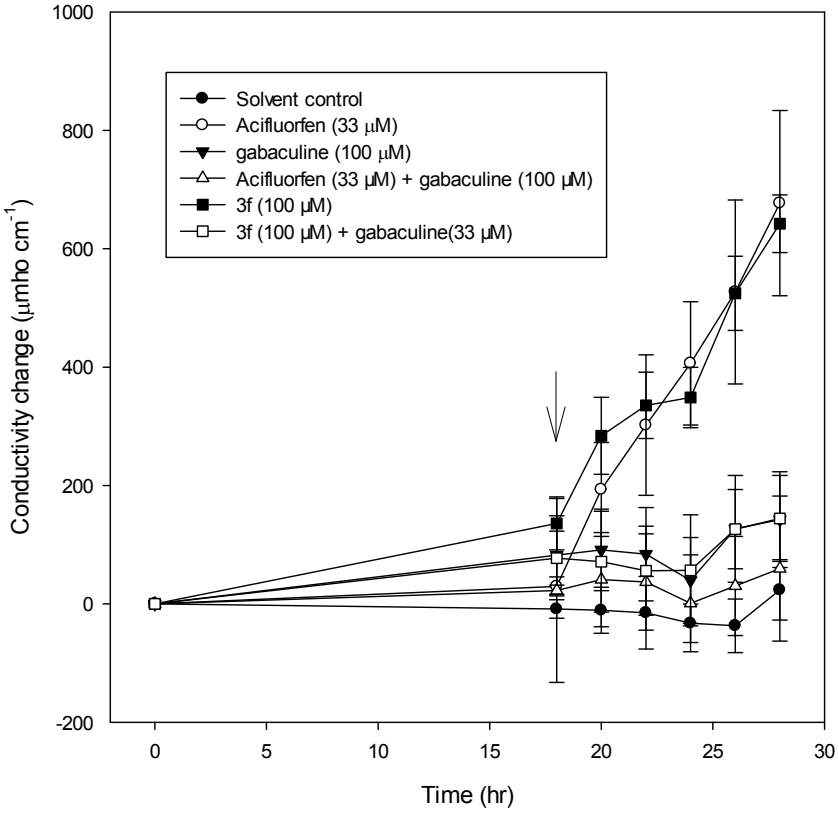

Figure 4. Effects of 100 μM gabaculine on the electrolyte leakage of cucumber cotyledon discs caused by 33 μM acifluorfen and 100 μM **3f**. The arrow indicates exposure to light.

Molecular Docking with PPO

From the electrolyte-leakage assay, the effects of compound **3f** were like that of a PPO inhibitor, so we conducted molecular modeling analysis of compound **3f** with *Nt*PPO. As shown in Figure **5a**, there were four π–π interactions between FAD and the quinoxaline ring with the distances of 6.3 Å, 7.0 Å, 5.0 Å, 5.5 Å respectively; second, there were two strong hydrogen bonding interactions (2.2 Å and 2.1 Å) between Thr176 of PPO and the N atom of the cyan group in the compound **3f** and Arg98 of PPO and the oxygen atom of the CH_3O group in compound **3f,** respectively. From the cocrystal (Figure **5b**), a strong hydrogen bond exists between Arg98 and the oxygen atom of a carbonyl group of **3f**. There are also π–π interactions between benzene ring of PPO inhibitor and Phe392 in the cocrystal. From the herbicide assay, **3f** caused leaf bleaching, and gabaculine-reversible electrolyte-leakage, indicating that it is a PPO inhibitor. However, it is weaker than the commercial PPO inhibitor acifluorfen. Its different activity may be attributable to the different π–π interactions.

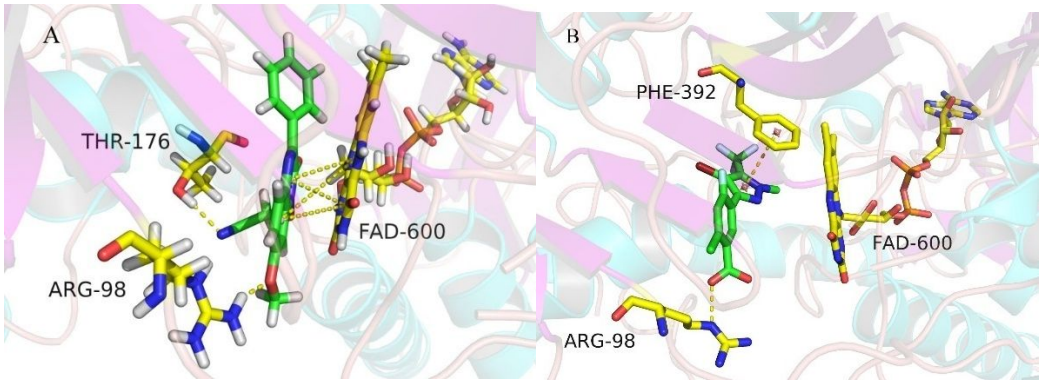

Figure **5**. Simulated binding modes of compound **3f** with *Nt*PPO(a) and complex binding modes in co-crystal.

Fungicidal Activity

313 With bioautographic methods, visible clear zones or diffuse zones observed after incubation and
314 the results were listed in Table 2 and Figure 6. All the seven quinoxaline compounds possessed
315 good fungicidal activity against strawberry anthracnose pathogens at the concentration tested,
316 especially compounds **3f** and **3g** (Table 2, Figure 6)**.** The activity against three species is the same
317 as the positive control, captan, at 20 μg/mL. Compounds **3b** and **3d** produced both clear and
318 diffuse inhibition zones for the *C. gloeosporioides* and *C. acutatum* (Table **2**). The diffuse zones
319 also had the good activity. From the fungicidal activity data, the trend of the compounds against
320 three fungi was *C. acutatum*>*C. gloeosporioides*>*C. fragariae*. Among these compounds, the
321 compounds with alkyl group still possessed the best activity against three fungi, whatever the clear
322 zone or diffuse zone**.** The (hetero-)aromatic substituted compounds exhibited weak activity against
323 *C. fragariae*. All the compounds displayed good activity against *C. acutatum*, except compound
324 **3c**, which is similar with the activity against *C. gloeosporioides*.
325
326 Table **2** The fungicidal activity against three fungi of seven compounds at 160 mg/spot

No.	inhibitory-zone diameter (mm)		
	C. acutatum	*C. fragariae*	*C. gloeosporioides*
3a	15	7	8
3b	8/15[a]	7	9/17[a]
3c	6[a]	6	6
3d	9/17[a]	10	10/16[a]
3e	13	7	13

3f	15	15	16
3g	18	16	19
captan	15	14	17
Solvent control(ethanol)	0	0	0

[a] Clear zone/Diffuse zone beyond the clear zone

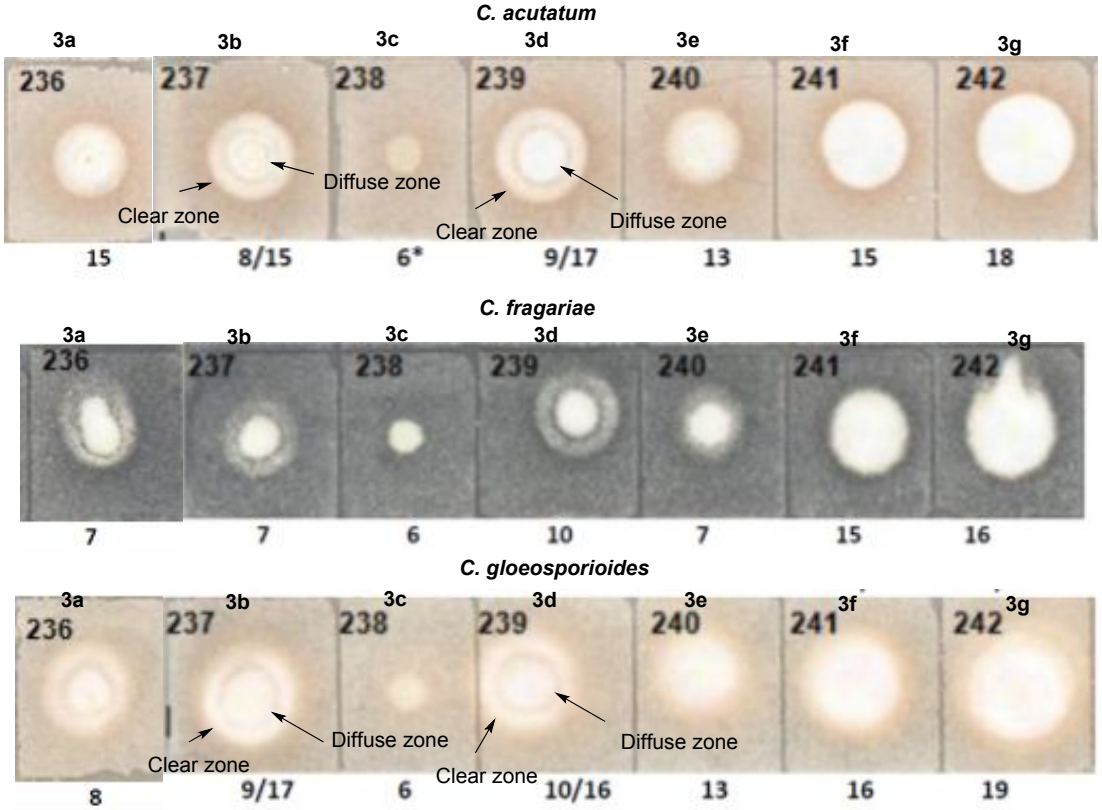

Figure **6** The inhibitor zone of compound **3a-3g** against three fungi.

Insecticidal Activity

All of the compounds were tested for mosquito larvicidal activity (Table **3**). Most of these compounds provided excellent larvicidal activity (100%) at 1 μg/μL, except for compounds **3d** and **3f**. When the concentration is at 0.5 μg/μL, the activities of compounds **3b** and **3g** are 100%, and compounds **3c** and **3e** also possessed good mosquito larvicidal activity (>90%). Compounds **3a** and **3f** exhibited moderate activity (>60%). Compounds **3c, 3e, 3f** and **3g** maintained good larvicidal activity (>60%), at 0.1 μg/μL. Negative controls produced no inseciticidal activity, whereas permethrin was highly mosquito larvicidal activity against 1st instar ORL strain (Table **3**). From the larvicidal activity data, the trend of the seven quinoxaline compounds against larvae was alkyl>heterocycle>substituted benzene. Among these compounds, the compounds with alkyl group still possessed the best activity against larvae, while the heterocyclic substituted compound and the 4-BrPhCH_2 also exhibited good activity at 0.1 μg/μL. But they still displayed weaker activity than that of positive control.

Table **3** The larvae activity against 1st instar ORL strain.

No.	1 μg/μL	0.5 μg/μL	0.25 μg/μL	0.1 μg/μL
3a	100	73.3 ± 30.6	66.7 ± 57.7	46.7 ± 41.6
3b	100	100	86.7 ± 11.5	46.7 ± 41.6
3c	100	93.3 ± 11.5	66.7 ± 30.6	60.0 ± 52.9
3d	73.3 ± 30.6	33.3 ± 41.6	20.0 ± 34.6	26.7 ± 30.6
3e	100	93.3 ± 11.5	73.3 ± 30.6	66.7 ± 57.7
3f	73.3 ± 46.2	66.7 ± 57.7	66.7 ± 57.7	60.0 ± 52.9

3g	100	100	100	80.0 ± 34.6
Untreated	0	0	0	0
Permethrin	100	100	100	100

348

349 ***DFT(B3LYP) Calculation***

350 HOMO, LUMO, energy gaps, ClogP and molecular total energy of low activity compound **3c** and

351 high activity compound **3f** are calculated using DFT method and the results are listed in Table **4**.

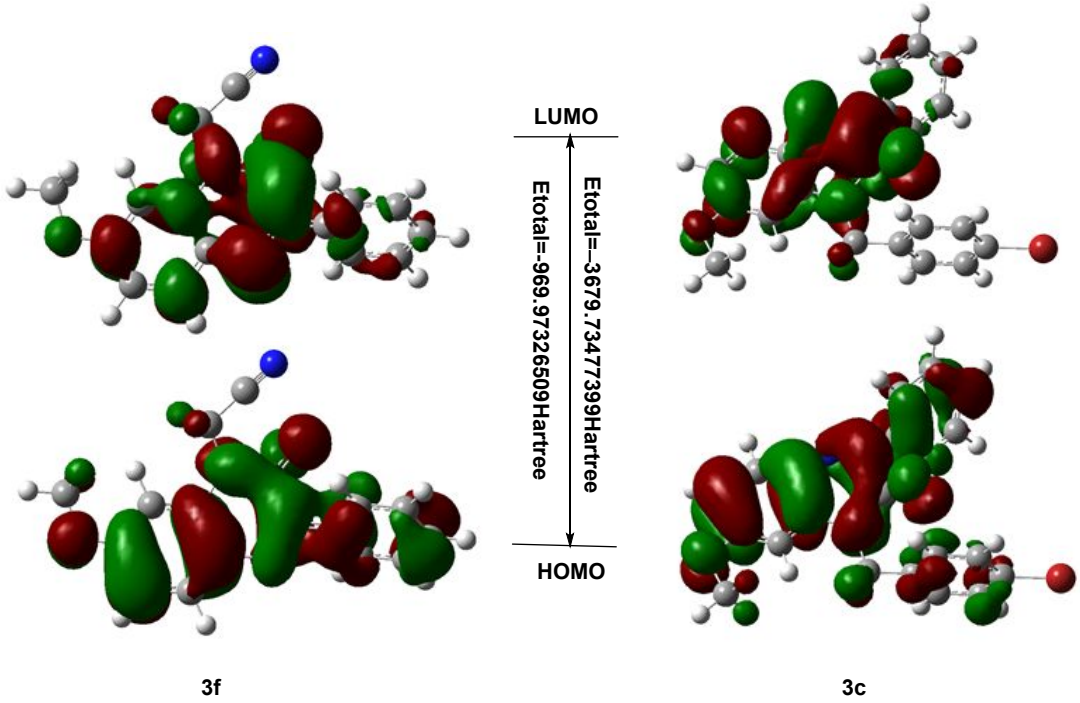

352

353 Figure 7 The HOMO and LUMO of compounds **3c** and **3f**

354

355 Frontier molecular orbital can supply information about electrons transfer, especially between the

356 HOMO and LUMO. The two orbitals' energy and the energy gap are important information for

357 mechanism of the molecules and target enzyme[44-45]. From Figure **7**, the compounds **3c** and **3f**

358 contain two parts: the quinoxaline ring and CH_2R-substituted group. For the compound **3c**, the

359 HOMO is located on the quinoxaline ring, benezene ring, 4-bromobenzene ring and CH_2 bridge,
360 But the LUMO is only located on the quinoxaline ring and CH_2 bridge. Hence, electron transfer of
361 compound **3c** is from the quinoxaline ring to the 4-bromobenzene ring via the CH_2 bridge and the
362 energy gap is 0.14975 Hartree. For the compound **3f**, the HOMO is mainly located on the
363 quinoxaline ring, benzene ring and CH_2 bridge, while the LUMO is located on the quinoxaline
364 ring and CH_2 bridge. The electron transition is on the quinoxaline ring and CH_2 bridge, and the
365 CN group does not contribute to the electron transition and the energy gap is 0.15065 Hartree. The
366 total energies of the two compounds are different: compound **3c** (-3679.73477399 Hartree) is
367 lower than compound **3f** (-969.97326509 Hartree). Also the ClogP values of the two compounds
368 differ. The ClogP of compound **3f** is 2.55843, while that of compound **3c** is 5.30123. The ClogP
369 also indicated that the substituted group on the N-quinoxaline ring can influence the bioactivity.
370 Furthermore, the FMO provided meaningful information as to lead compound of this new family
371 of PPO inhibitor that will be useful to design more potential lead compounds in the future.

372

373 **Table 4.** Total energy, HOMO, LUMO and energy gap, CLogP.

Energy	3c	3f
E_{total}/Hartree [b]	-3679.73477399	-969.97326509
E_{HOMO}/Hartree	-0.21662	-0.22443
E_{LUMO}/Hartree	-0.06687	-0.07378
ΔE [a]/Hartree	0.14975	0.15065
CLogP	5.30123	2.55843

374

375

Acknowledgements

This work was supported by Zhejiang Provincial Natural Science Foundation of China (No. LY19C140002), Research Fund of Department of Education of Zhejiang Province (Y201941832). We thank Drs. James J. Becnel and Alden Estep for evaluating larvicidal activity and Solomon Green, Jesse Linda Robertson and Robert Johnson for their technical assistance.

References

(1). Zhang, C.; Kong, L.; Lei, X.; Deng, Z.; You, D. Advance in the research on quinomycins biosynthesis. *Chin. J. Org. Chem.* **2014**, *34*, 1240-1252.

(2). Abdelfattah, M.S.; Kazufumi, T.; Ishibashi, M. Izumiphenazines A-C: Isolation and structure elucidation of phenazine derivatives from *Streptomyces sp.* IFM 11204. *J. Nat. Prod.* **2010,** *73,* 1999-2002.

(3). Henriques, B.J.; Olsen, R.K.; Bross, P.; Gomes, C.M. Emerging roles for riboflavin in functional rescue of mitrochondrial beta-oxidation flavoenzymes. *Curr. Med. Chem.* **2010**, *17*, 3842-3854.

(4). Shingare, R.D.; Velayudham, R.; Gawade,J.R.; Reddy, D. S. First total synthesis of hunanamycin A. *Org. Lett.* **2013**, *15,* 4556-4559.

(5). Hu, Y.; Wang, K.; MacMillan, J.B. Hunanamycin A, an antibiotic from amarine-derived *Bacillus hunanensis*. *Org. Lett.* **2013**, *15*, 390-393.

(6). Refat, M.S.; Moussa, M.A.A.; Mohamed, S.F. Synthesis, spectroscopic characterization, thermal analysis and electrical conductivity studies of Mg(II), Ca(II), Sr(II) and Ba(II) vitamin B2 complexes. *J. Mol. Struct.* **2011**, *994*, 194-201.

(7). Ahmed, H.E.A.; Ihmaid, S.K.; Omar, A.M.; Shehata, A.M.; Rateb, H.S.; Zayed,M.F.; Ahmed, S.; Elaasser, M.M. Design, synthesis, molecular docking of new lipophilic acetamide derivatives affording potential anticancer and antimicrobial agents. *Bioorg. Chem.* **2018**, *76*, 332-342.

(8). Loughran, H.M.; Han, Z.; Wrobel, J.E.; Decker, S.E.; Ruthel, G.; Freedman, B.D.; Harty, R.N.; Reitz,A.B. Quinoxaline-based inhibitors of ebola and Marburg VP40 egress. *Bioorg. Med. Chem. Lett.* **2016**, *26*, 3429-3435.

(9). Ibrahim, M.K.; Eissa, I.H.; Abdallah, A.E.; Metwaly, A.M.; Radwan, M.M.; ElSohly, M.A. Design, synthesis, molecular modeling and anti-hyperglycemic evaluation of novel quinoxaline derivatives as potential PPARc and SUR agonists. *Bioorg. Med. Chem.* **2017**, *25*, 1496-1513.

(10). Achutha, L.; Parameshwar, R.; Reddy, B.M.; Babu, H.V. Microwave-assisted synthesis of some quinoxaline-incorporated Schiff bases and their biological evaluation. *J. Chem.* **2013**, *2013*, 578438.

(11). Carta, A.; Sanna, P.; Gherardini, L.; Usai, D.; Zanetti, S. Novel functionalized pyrido[2,3-g]quinoxalinones as antibacterial, antifungal and anticancer agents, *Farmaco* **2001,** *56*, 933-938.

(12). Shekhar, A.C.; Rao, P.S.; Narsaiah, B.; Allanki, A.; Sijwali, P.S. Emergence of pyrido quinoaxalines as a new family of antimalarial agents. *Eur. J. Med. Chem.* **2014**, *77*, 280-287.

(13). Ali, I.; Lee, J.; Go, A.; Choi, G.; Lee, K. Discovery of novel [1,2,4]triazolo[4,3-a]quinoxaline aminophenyl derivatives as BET inhibitors for cancer treatment. *Bioorg. Med. Chem. Lett.* **2017**, *27*, 4606-4613.

(14). Corona, P.; Carta, A.; Loriga, M.; Vitale, G.; Paglietti, G. Synthesis and in vitro antitumor activity of new quinoxaline derivatives. *Eur. J. Med. Chem.* **2009**, *44*, 1579-1591.

(15). Sonawane, N.D.; Rangnekar, D.W. Synthesis and application of 2-styryl-6,7-dichlorothiazolo[4,5-b]-quinoxaline based fluorescent dyes: Part 3, *J. Heterocycl. Chem.* **2002,** *39*, 303-308.

(16). Toshima, K.; Takano, R.; Ozawa, T.; Matsumura, S. Molecular design andevaluation of quinoxaline-carbohydrate hybrids as novel and efficient photoinduced GG-selective DNA cleaving agents. *Chem. Commun.* **2002,** *2*, 212-213.

(17). Low, C.M.; Fox, K.R.; Waring, M.J. DNA sequence selectivity of three biosynthetic analogues of the quinoxaline antibiotics. *Anticancer Drug Des.* **1986,** *1*, 149-160.

(18). Waring, M.; Ben-Hadda, T.; Kotchevar, A.; Ramdani, A.; Touzani, R.; Elkadiri, S.; Hakkou, A.; Bouakka, M.; Ellis, T. 2,3-Bifunctionalized quinoxalines: synthesis, DNA interactions and evaluation of anticancer, anti-tuberculosis and antifungal activity. *Molecules* **2002,** *7*, 641.

(19). Gokul Raj, K.; Manikandan, R.; Arulvasu, C.; Pandi, M. Anti-proliferative effect of fungal taxol extracted from *Cladosporium oxysporum* against human pathogenic bacteria and human colon cancer cell line HCT 15, *Spectrochim. Acta A Mol. Biomol. Spectrosc.* **2015,** *138*, 667-674.

(20). Lilly & Co Eli, Inhibiting plant growth with 3-phenyl quinoxalines. US3582315-A, **1971.**

(21). Lilly & Co Eli, 2-piperidino-3-phenylquinoxalines and 6- or 7-substd derivs-selecti preemergence herbicides. US3647793-A, **1972**.

(22). Schaper, W.; Willms, L.; Rosinger, C.; Hacker, E.; Rose, E.; Schmutzler, D. Protecting useful plants or crop plants against phytotoxic side effects of agrochemicals comprises applying new or known 1,2-dihydroquinoxalin-2-one derivatives as safener. US2005256000-A1, **2005.**

(23). Min, L.J.; Zhai, Z.W.; Shi, Y.X.; Han, L.; Tan, C.X.; Weng, J.Q.; Li, B.J.; Zhang, Y.G.; Liu, X.H. Synthesis and biological activity of acyl thiourea containing difluoromethyl pyrazole motif. *Phosphorus Sulfur Silicon Relat. Elem.* **2020**, *195*, 22-28.

(24). Liu, X.H.; Qiao, L.; Zhai, Z.W.; Cai, P.P.; Cantrell, C.L.; Tan, C.X.; Weng, J.Q.; Han, L.; Wu, H.K. Novel 4-pyrazole carboxamide derivatives containing flexible chain motif: Design, synthesis and antifungal activity. *Pest Manag. Sci.* **2019**, *75*, 2892-2900.

(25). Fu, Q.; Cai, P. P.; Cheng, L.; Zhong, L. K.; Tan, C. X.; Shen, Z. H.; Han, L.; Liu, X. H. Synthesis and herbicidal activity of novel pyrazole aromatic ketone analogs as HPPD inhibitor. *Pest Manag. Sci.* **2020**, *76*, 868-879

(26). Wang, H.; Zhai, Z.W.; Shi, Y.X.; Tan, C.X.; Weng, J.Q.; Han, L.; Li B.J.; Liu, X.H. Novel trifluoromethylpyrazole acyl thiourea derivatives: Synthesis, antifungal activity and docking study. *Lett. Drug Des. Discov.***2019**, *16,* 785-791.

(27). Cheng, L.; Zhang, R.R.; Wu, H.K.; Xu, T.M.; Liu, X.H. The synthesis of 6-(tertbutyl)-8-fluoro-2,3-dimethylquinoline carbonate derivatives and their antifungal activity against pyricularia oryzae, *Front. Chem. Sci. Eng.* **2019**, *13*, 369-376.

(28). Zhai, Z.W.; Wang, Q.; Shen, Z.H.; Tan, C.X.; Weng, J.Q.; Liu, X.H. Synthesis and biological activity of 1,2,4-triazole thioether derivatives containing pyrazole moiety. *Chin. J. Org. Chem.* **2017**, *37*, 232-236.

(29). Fang, Y.M.; Zhang, R.R.; Shen, Z.H.; Tan, C.X.; Weng, J.Q.; Xu, T.M.; Liu, X.H. Huang, H.Y.; Wu, H.K. Synthesis and antifungal activity of some 6-*tert*-butyl-8-chloro-2, 3-dimethylquinolin-4-ol derivatives against *Pyricularia oryae*. *Lett. Drug Des. Discov.* **2018**, *15*, 1314-1318.

(30). Hua, X.W.; Liu, W.R.; Su, Y.Y.; Liu, X. H.; Liu, J.B.; Liu, N.N. Wang, G.Q.; Jiao, X.Q.; Fan, X.Y.; Xue, C.M.; Liu, Y.; Liu, M. Studies on the Novel Pyridine Sulfide Containing SDH Based Heterocyclic Amide Fungicide. *Pest Manag. Sci.* **2020**, doi: 10.1002/ps.5773.

(31). Liu, X.H.; Fang, Y.M.; Xie, F.; Zhang, R.R.; Shen, Z.H.; Tan, C.X.; Weng, J.Q.; Xu, T.M.; Huang, H.Y. Synthesis and in vivo fungicidal activity of some new quinoline derivatives against rice blast. *Pest Manag. Sci.* **2017**, *73*, 1900-1907.

(32). Liu, X.H.; Zhao, W.; Shen, Z.H.; Xing, J.H.; Xu, T.M.; Peng, W.L. Synthesis, nematocidal activity and SAR study of novel difluoromethylpyrazole carboxamide derivatives containing flexible alkyl chain moieties. *Eur. J. Med. Chem.* **2017**, *125*, 881-889.

(33). Liu, X.H.; Xu, X.Y.; Tan, C.X.; Weng, J.Q.; Xin, J.H.; Chen, J. Synthesis, crystal structure, herbicidal activities and 3D-QSAR study of some novel 1,2,4-triazolo[4,3-a]pyridine derivatives. *Pest Manag. Sci.* **2015**, *71*, 292-301.

(34). Jin, T.; Zhai, Z.W.; Han, L.; Weng, J.Q.; Tan, C.X.; Liu, X.H. Synthesis, crystal structure, docking and antifungal activity of a new pyrazole acylurea compound. *Chin. J. Struct. Chem.* **2018**, *37*, 1259-1264.

(35). Dayan, F.E.; Romagni, J.G.; Duke, S.O. Investigating the mode of action of natural phytotoxins. *J. Chem. Ecol.* **2000**, *26*, 2079-2094.

(36). Michel, A.; Johnson, R.D.; Duke, S.O.; Scheffler, B.E. Dose-response relationships between herbicides with different modes of action and growth of *Lemna paucicostata*: An improved exotoxicological method. *Environ. Toxicol. Chem*. **2004**, *232*, 1074-1079.

(37). R-Development-Core-Team. R: A Language and Environment for Statistical Computing; 3.2.4 Version; R Foundation for Statistical Computing: Vienna, Austria, **2015**.

(38). Dayan, F.E.; Watson, S.B. Plant cell membrane as a marker for light-dependent and light-independent herbicide mechanisms of action. *Pestic. Biochem. Physiol.* **2011**, *101*, 182-190.

(39). Lydon, J.; Duke, S.O. Porphyrin synthesis is required for photobleaching activity of the *p*-nitrosubstituted diphenyl either herbicides. *Pesti.c Biochem. Physiol.* **1988**, *31*, 74-83

(40). Wedge, D.E.; Nagle, D.G.A. New 2D-TLC bioautography method for the discovery of novel antifungal agents to control plant pathogens. *J. Nat. Prod.* **2000**, *63*, 1050-1054.

(41). Liu, X.H.; Wang, Q.; Sun, Z.H.; Wedge, D.E.; Becnel, J.J.; Estep, A.S.; Tan, C.X.; Weng, J.Q. Synthesis and insecticidal activity of novel pyrimidine derivatives containing urea pharmacophore against *Aedes aegypti. Pest Manag. Sci.* **2017**, *73*, 953-959.

(42). Pridgeon, J.W.; Becnel, J.J.; Clark, G.G.; Linthicum, K.J. A high-throughput screening method to identify potential pesticides for mosquito control. *J. Med. Entomo.* **2009,** *46*, 335-341.

(43). Chang, F.; Dutta, S.; Becnel, J.J.; Estep, A.S.; Mascal, M. Synthesis of the insecticide prothrin and its analogues from biomass-derived 5-(chloromethyl) furfural. *J. Agr. Food Chem.* **2014**, *62*, 476-480.

(44). Shen, Z.H.; Sun, Z.H.; Becnel, J.J.; Estep, A.; Wedge, D.E.; Tan, C.X.; Weng, J.Q.; Han, L., Liu. X.H. Synthesis and mosquiticidal activity of novel hydrazone containing pyrimidine derivatives against *Aedes aegypti*. *Lett. Drug Des. Discov.* **2018**, *15*, 951-956.

(45). Frisch, M.-J.; Trucks, G.-W.; Schlegel, H.-B.; Scuseria, G.-E.; Robb, M.-A.; Cheeseman, J.-R.; Montgomery, J.-A. Jr.; Vreven, T.; Kudin, K.-N.; Burant, J.-C.; Millam, J.-M.; Iyengar, S.-S.; Tomasi, J.; Barone, V.; Mennucci, B.; Cossi, M.; Scalmani, G.; Rega, N.; Petersson, G.-A.; Nakatsuji, H.; Hada, M.; Ehara, M.; Toyota, K.; Fukuda, R.; Hasegawa, J.; Ishida, M.; Nakajima, T.; Honda, Y.; Kitao, O.; Nakai, H.; Klene, M.; Li, X.; Knox, J.-E.; Hratchian, H.-P.; Cross, J.-B.; Adamo, C.; Jaramillo, J.; Gomperts, R.; Stratmann, R.-E.; Yazyev, O.; Austin, A.-J.; Cammi, R.; Pomelli, C.; Ochterski, J.-W.; Ayala, P.-Y.; Morokuma, K.; Voth, G.-A.; Salvador, P.; Dannenberg, J.-J.; Zakrzewski, V.-G.; Dapprich, S.; Daniels, A.-D.; Strain, M.-C.; Farkas, O.; Malick, D.-K.; Rabuck, A.-D.; Raghavachari, K.; Foresman, J. B.; Ortiz, J. V.; Cui, Q.; Baboul, A. G.; Clifford, S.; Cioslowski, J.; Stefanov, B.-B.; Liu, G.; Liashenko, A.; Piskorz, P.; Komaromi, I.; Martin, R.-L.; Fox, D.-J.; Keith, T.; Al-Laham, M.-A.; Peng, C.-Y.; Nanayakkara, A.; Challacombe, M.; Gill, P.-M.-W.; Johnson, B.; Chen, W.; Wong, M.-W.; Gonzalez, C.; Pople, J.-A. Gaussian 03, Revision C. 01, Gaussian, Inc., Wallingford CT, **2004.**

523 Tables and Figures

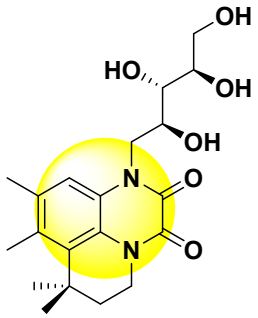

Hunanamycin A

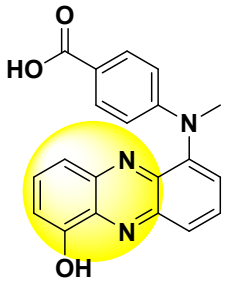

Izumiphenazine C

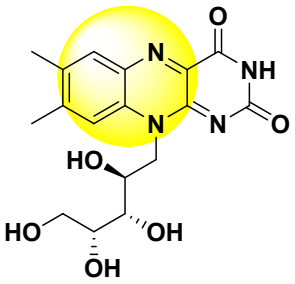

Vitamin B2

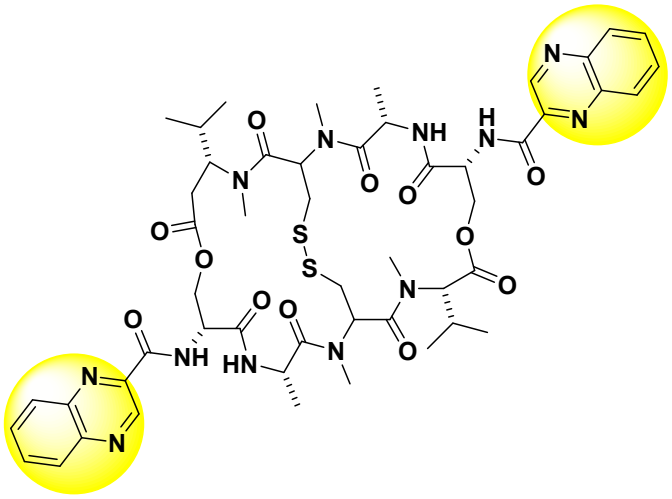

triostin A

524

525 Figure **1** Some natural products with the quinoxaline moiety

526

527

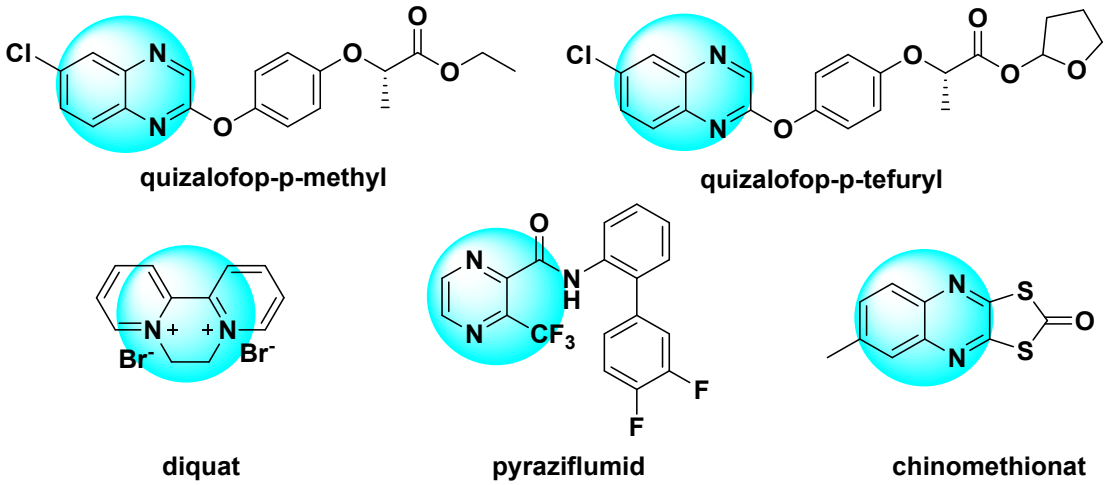

528

529

530

531 Figure 2 Representative pesticides with the pyrazine moiety

532

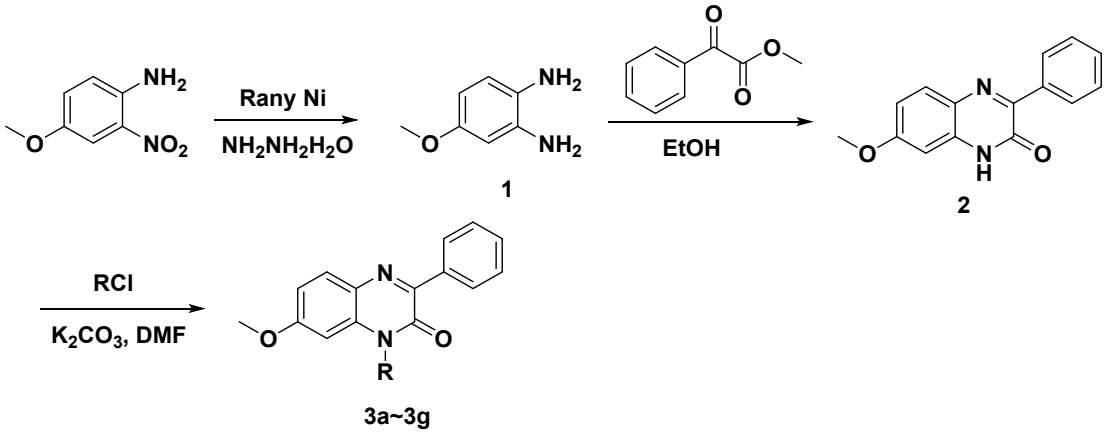

533

534 Scheme 1. The synthetic pathway of quinoxaline derivatives

535

536

537

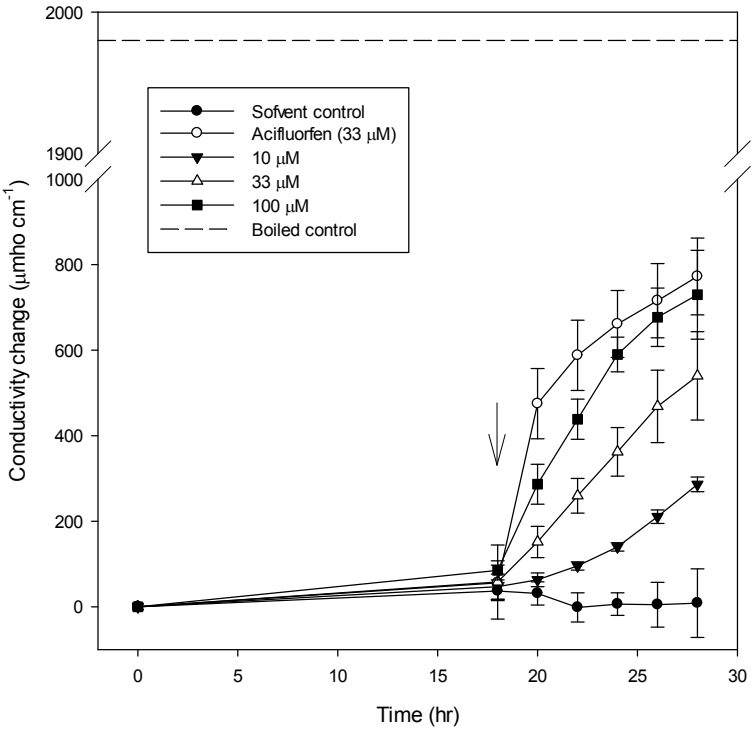

538

539 Figure 3. The electrolyte-leakage of cucumber cotyledon discs caused by compound **3f** at different

540 concentrations. The arrow indicates exposure to light. Error bars are ± 1SE. Dotted line is

541 conductivity of boiled discs (maximum possible effect).

542

543

544

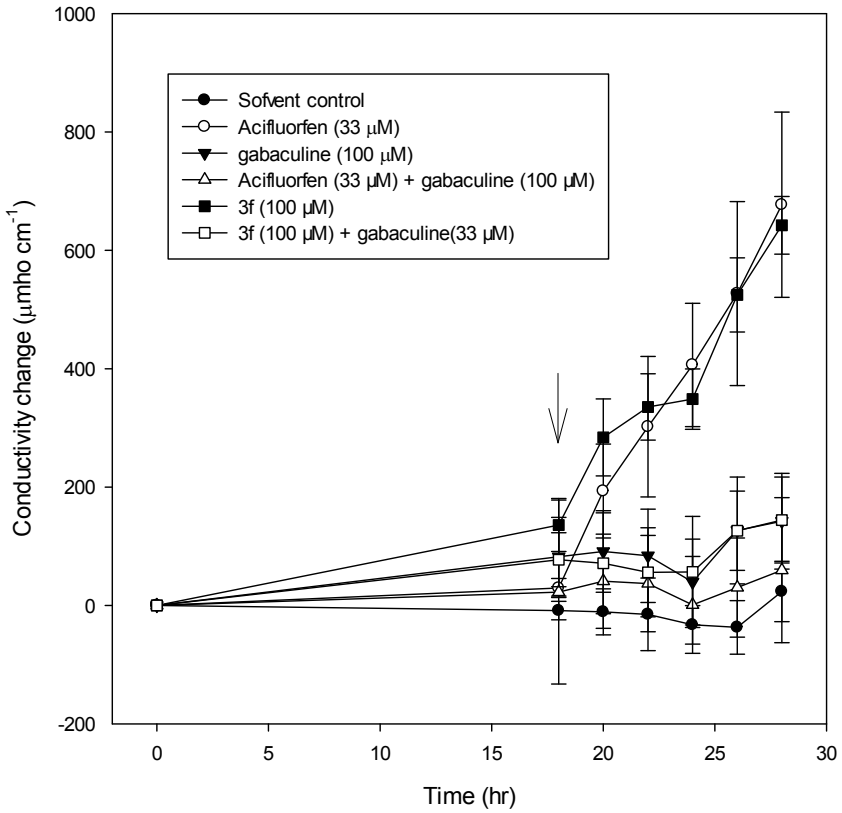

545

546 Figure 4. A. Effects of 100 μM gabaculine on the electrolyte leakage of cucumber cotyledon

547 discs caused by 33 μM acifluorfen and 100 μM **3f**. The arrow indicates exposure to light.

548

549

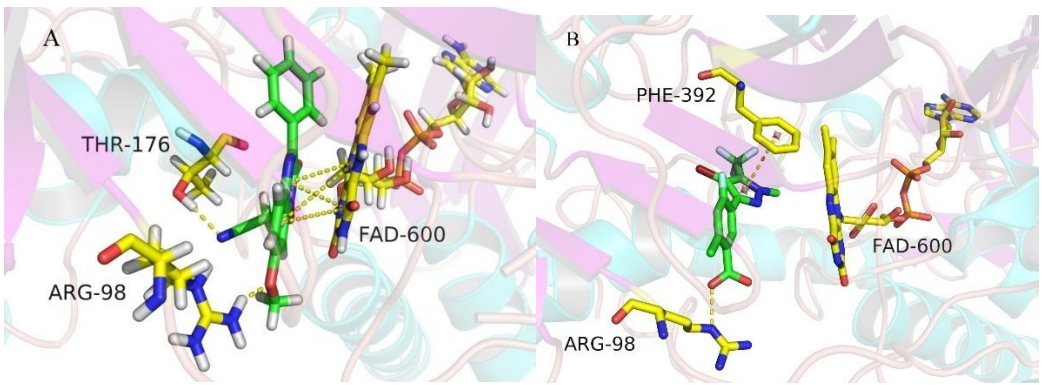

550

551 Figure **5**. Simulated binding modes of compound **3f** with *Nt*PPO(a) and complex binding modes in

552 co-crystal.

553

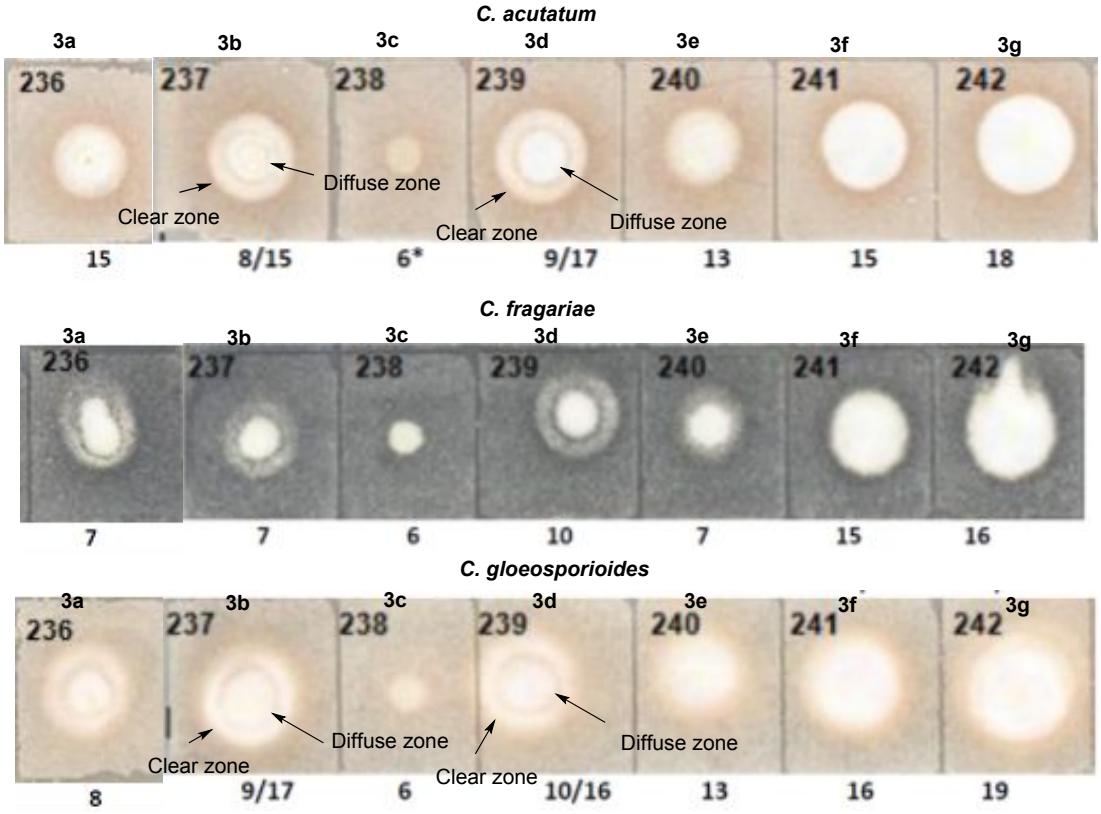

554

555

556 Figure **6** The inhibitor zone of compound **3a-3g** against three fungi.

557

558

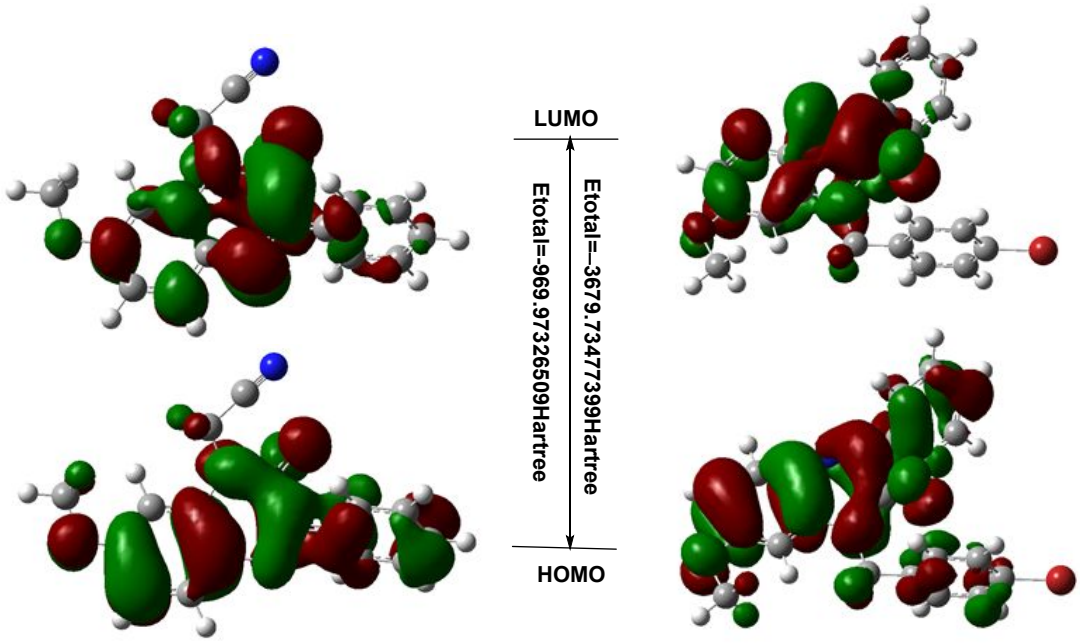

559

560 Figure 7 The HOMO and LUMO of compounds **3c** and **3f**

561

562

563 Table **1** The phytotoxicity of seven compounds against three plant species

No.	R	Lettuce	Agrostis	Duckweed(IC_{50} (μM))
3a	4-CNPhCH_2	3	1	-
3b	4-*t*-BuPhCH_2	3	1	-
3c	4-Br PhCH_2	2	1	-
3d	3-CNPhCH_2	4	3	-
3e	2-Cl-thiazole-5-CH_2	4	3	-
3f	CH_2CN	5*	4	13.99±3.17
3g	CH_2=$CHCH_2$	5	4	24.56±10.02
Clomazone		5	5	126.10 ± 18.87

Acifluorfen	5	5	0.73 ± 0.09

564 0 = no effect and 5 = no germination of the seeds.

565 *bleached

566

567

568 Table **2** The fungicidal activity against three fungi of seven compounds at 20 μg/mL

No.	inhibitory-zone diameter (mm)		
	C. acutatum	*C. fragariae*	*C. gloeosporioides*
3a	15	7	8
3b	8/15[a]	7	9/17[a]
3c	6[a]	6	6
3d	9/17[a]	10	10/16[a]
3e	13	7	13
3f	15	15	16
3g	18	16	19
captan	15	14	17

569 [a] Clear zone/Diffuse zone beyond the clear zone

570

571

572 Table **3** Percent mortality after 24 h for 1st instar ORL strain.

No.	1 μg/μL	0.5 μg/μL	0.25 μg/μL	0.1 μg/μL
3a	100	73.3 ± 30.6	66.7 ± 57.7	46.7 ± 41.6

3b	100	100	86.7 ± 11.5	46.7 ± 41.6
3c	100	93.3 ± 11.5	66.7 ± 30.6	60 ± 52.9
3d	73.3 ± 30.6	33.3 ± 41.6	20 ± 34.6	26.7 ± 30.6
3e	100	93.3 ± 11.5	73.3 ± 30.6	66.7 ± 57.7
3f	73.3 ± 46.2	66.7 ± 57.7	66.7 ± 57.7	60 ± 52.9
3g	100	100	100	80 ± 34.6
Untreated	0	0	0	0
Permethrin	100	100	100	100

573

574

575 **Table 4.** Total energy and frontier orbital energy.

Energy	**3c**	**3f**
E_{total}/Hartree [b]	-3679.73477399	-969.97326509
E_{HOMO}/Hartree	-0.21662	-0.22443
E_{LUMO}/Hartree	-0.06687	-0.07378
ΔE [a]/Hartree	0.14975	0.15065
CLogP	5.30123	2.55843

576

577

578

579 Table of Contents Graphic

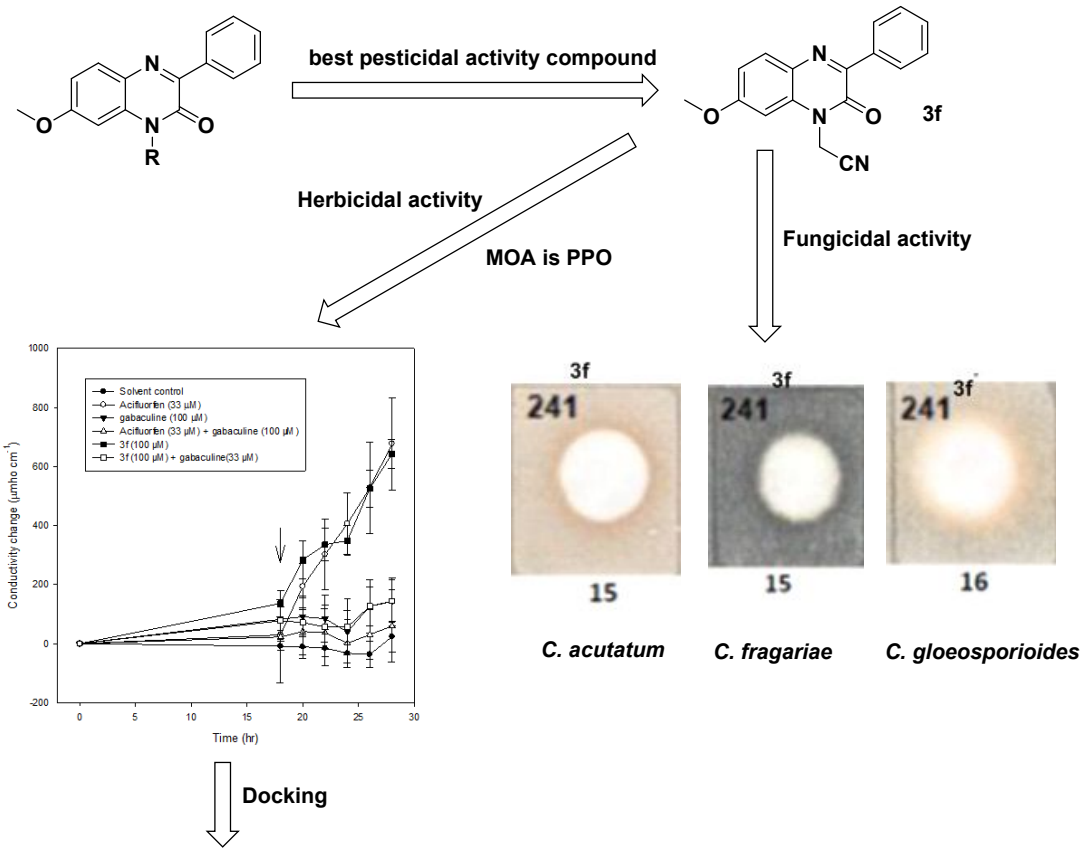

580

581